Evidence for solution-mediated phase transitions in kidney stones -Phase transition exacerbates kidney stone disease-

Mihoko Maruyama[1,2], Yutaro Tanaka[3], Koichi Momma[4], Yoshihiro Furukawa[5], Hiroshi Y. Yoshikawa[1], Rie Tajiri[6], Masanori Nakamura[7], Kazumi Taguchi[3], Shuzo Hamamoto[3], Ryosuke Ando[3], Katsuo Tsukamoto[5], Kazufumi Takano[2], Masayuki Imanishi[1], Shigeyoshi Usami[1], Kenjiro Kohri[3], Atsushi Okada[3], Takahiro Yasui[3], Masashi Yoshimura[8], Yusuke Mori[1]*

*Corresponding author: maruyama@eei.eng.osaka-u.ac.jp

1. Graduate School of Engineering, Osaka University, 2-1, Yamadaoka, Suita 565-0871, Japan

2. Graduate School of Life and Environmental Sciences, Kyoto Prefectural University, 1-5, Hangi-cho, Shimogamo, Sakyo-ku, Kyoto, Kyoto 606-8522, Japan

3. Department of Nephro-urology, Nagoya City University Graduate School of Medical Sciences, 1-Kawasumi, Mizuho-cho, Mizuho-Ku Nagoya 467-8601, Japan

4. National Museum of Nature and Science, 4-1-1 Amakubo, Tsukuba 305-0005, Japan

5. Department of Earth Science, Tohoku University, 6-3 Aza-Aoba, Aramaki, Aoba-ku, Sendai 980-8578, Japan

6. Tajiri Thin Section Laboratory, 3-1-11 Sannose, Higashiosaka, Osaka 577-0849, Japan

7. Nagoya Institute of Technology, Gokiso-cho, Showa-ku, Nagoya, Aichi, 466-8555 Japan

8. Institute of Laser Engineering, Osaka University, 2-6, Yamadaoka, Suita City, Osaka 565-0871 Japan

ABSTRACT

In this study, we investigated calcium oxalate (CaOx) kidney stones and showed direct evidence of the solution-mediated phase transition of calcium oxalate dihydrate (COD; the metastable phase) to calcium oxalate monohydrate (COM; the stable phase). We examined the crystal phases, crystal textures, and protein distributions within thin sections of calcium oxalate kidney stones. Observation with a polarized-light microscope showed that the outline of the mosaic texture, in which COM crystals are assembled in a mosaic pattern, roughly coincides with COD's crystallographically stable face angles. Microfocus X-ray CT measurement captured the intermediate process of the phase transition, starting inside the COD single crystal and gradually transforming to COM crystals. In addition, the distribution of osteopontin and prothrombin fragment-1, common proteins contained in urine and visualized by multicolor fluorescence immunostaining, showed no apparent striations inside the COM single crystals with the mosaic texture, although the striation is apparent inside the COD single crystals. This is probably because the phase transition of mosaic-like COM occurred in a semi-closed system inside the COD single crystal, so the effect of periodic (day-night, seasonal, etc.) urinary protein concentration changes was small. On the other hand, striations were visible in concentrically laminated COM. This indicated that concentrically laminated COM formed in response to the changes in urinary protein concentrations. From the above, we conclude that the COD single crystals and the concentrically laminated COM

seen in CaOx stones are primary structures, and the mosaic COM is a secondary structure that is a pseudomorph formed by the solution-mediated phase transition from COD single crystals.

Introduction

Kidney stone disease is a common and severe disorder in which hard deposits or stones form in the kidneys and induce pain when flowing through the urinary tract (kidneys, ureters, bladder, and urethra).[1] The number of patients with the disease is increasing, and the recurrence rate at five years after diagnosis is exceptionally high at ≥45%. The condition is serious because repeated recurrences can lead to deterioration of renal function, which is ultimately life-threatening.[2 3] In order to prevent such recurrences, further elucidation of the stone formation process is urgently needed. Accordingly, various efforts have been made to clarify stone formation, such as examining the crystal components that make up kidney stones and the types of proteins contained therein.[1 4]

A kidney stone is composed of various excretory components in the urine. About 10% of a stone consists of organic substances called matrix (glycoproteins of 1 kDa or more). Although this is a small amount, these organic substances are deeply involved in stone formation. The remaining 90% or more are calculi-constituting salts (crystalline components), including calcium oxalate (CaOx), calcium phosphate (CaP), magnesium ammonium phosphate, uric acid, cystine, and other phases. CaOx is the major component, accounting for more than 70% of

total kidney stone components. CaOx has four pseudo-polymorphs: anhydrate, monohydrate (COM), dihydrate (COD), and trihydrate (COT).[5 6 7] COM and COD are often found in stones, and COT is rarely found. In the urinary environment, COM is the thermodynamically stable phase, and COD is the metastable phase.[8] Figure 1 shows the typical crystallographic morphology of COM and COD, using the COM and COD crystallographic data of Ref. [9]. We calculated the crystal morphologies as described in Refs. [10 11].

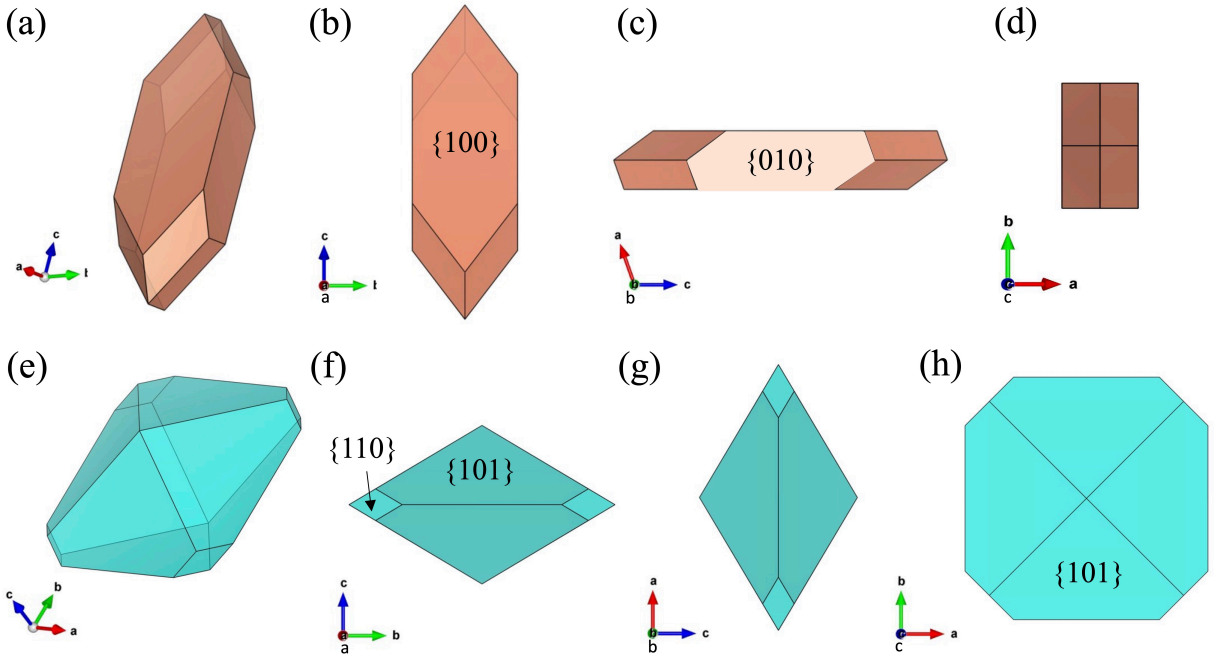

Figure 1. Typical morphologies of a COM crystal and a COD crystal predicted from each crystal structure. (a)-(d) Morphology of a monoclinic COM crystal. (e)-(h) Morphology of a tetragonal COD crystal. (a), (e) Projection from a direction that makes it easy to grasp the overall shape. (b), (f) Morphology seen from the a-axis direction. (c), (g) Morphology seen from the b-axis direction. (d), (h) Morphology viewed from the c-axis direction.

From a clinical viewpoint, evaluating the crystalline components of expelled stones is crucial because COD-based stones tend to recur easily.[12] From empirical viewpoint of medical practice, there are reports that COM stones are difficult to crush by surgery.[13] In addition, detailed analysis of kidney stones has shown that COD crystals are often larger than COM crystals. In the same report, the authors observed that COD crystals tend to exist around the periphery and COM crystals tend to exist around the center of kidney stones.[14] Recently, Sivagru et al. reported evidence of the dissolution of crystals in kidney stones.[15] Their findings are attracting a great deal of attention because the possibility of dissolving kidney stones within the body would greatly expand the number of potential new treatments. The authors considered that the dissolution of COD crystals involved a phase transition of COD crystals to COM crystals. Several earlier reports came to the same conclusion by observing kidney stone textures. [16] [17]

From the viewpoint of crystal growth, the relationship between the thermodynamically stable and metastable phases of crystals is significant. For example, in the crystal nucleation process, the metastable phase preferentially nucleates when the solution concentration is supersaturated with both the stable and metastable phases.[18] In addition, when the stable phase is grown using a solution-mediated phase transition, the growth rate is often faster than by direct growth of the stable phase from solution. As described above, in the kidney stone formation mechanism, the phase transition process from the metastable phase to the stable phase clearly affects the crystal nucleation and crystal growth processes. Zhang et al. examined the phase transition of calcium phosphate (CaP) and reported the underlying role

of a metastable phase of CaP, brushite, in the pathological mineralization of hydroxyapatite.[19] Díaz-Soler et al. focused on the nucleation of CaOx and suggested the importance of understanding the initial stages of mineralization to present a prevention strategy.[20] Furthermore, recent advances in analysis using atomic force microscopy, advanced scanning, and transmission microscopies enable nanoparticle imaging, and have become powerful approaches to understanding the phase transition. Many advancing research focuses on the initial nucleation and phase transition stages of CaOx, CaP and other biominerals.[21] Thus, clarifying the phase transition process in kidney stones is extremely important. In this study, we analyzed three samples from a Nagoya City University collection of kidney stones excreted from patients and found evidence suggesting that the solution-mediated phase transition is underway in kidney stones.

Materials and Methods

Ethics Statement

The institutional review board approved the research project presented in this paper of the Graduate School of Medicine, Nagoya City University. All methods were carried out following the relevant guidelines and regulations. Written informed consent was obtained from all subjects according to the procedures approved by the ethical committee board.

Sample preparation

CaOx kidney stones were selected from a collection of thousands of human kidney stones from the Department of Nephro-Urology, Nagoya City University, Japan. We prepared thin sections of three samples (nos. 1009-3, 1010-2 and 1011) with thicknesses of 20–30 μm using the resin-embedding method. The details are shown in Ref.[22] and Ref.[23].

Observation by a microfocus X-ray CT system

We identified the crystal components in the kidney stones using a microfocus X-ray CT system (inspeXio SMX-100CT Plus). The measurement parameters for the X-ray tube were 90 kV and 44 mA, with a voxel size of 0.005 mm/voxel. We measured samples 1011 and 1010-2 without any special processing. The main components of CaOx kidney stones, COM and COD, exhibit different amounts of X-ray absorption[24]. Therefore, approximate local phase identification was performed based on the differences in the values.

Crystal phase identification

We observed the size, coloration, and extinction of crystals in the kidney stone thin section using a polarized-light microscope (OPTIPHOT2-POL; Nikon), switching between open-Nicol and cross-Nicol prisms. This observation can visualize the unique structure and alignment of crystals in kidney stones.

We analyzed thin sections of sample1003-9 using an FT-IR microscope (FT/IR-6100; JASCO). The reflection method was used for measurement. The settings were as follows: cumulative number, 256; measurement range, 600 – 4000 cm^{-1}, measurement area, 50×50 μm.

Because the obtained specular reflection spectrum was affected by the anomalous dispersion of the refractive index, we performed a Kramers–Kronig[25] transformation after removing the absorption of H_2O and CO_2 in the atmosphere. We identified the CaOx phase (COM, COD) of each area by the method of Ref. [26].

Multicolor immunofluorescent staining of the protein matrix

The stone sections used to analyze mineral phases were also used to visualize protein distributions with multicolor immunofluorescent staining (Multi-IF staining). The primary antibodies used were mouse monoclonal anti-calgranulin A (1:100 dilution, sc-48352; Santa Cruz Biotechnology), rabbit polyclonal anti-osteopontin (1:100 dilution, sc-20631; Santa Cruz Biotechnology), and sheep monoclonal anti-human prothrombin Fragment 1 (1:500 dilution, CL20111AP; Cedarlane, Ontario, Canada). The fluorescently conjugated secondary antibodies used were anti-rabbit IgG(H+L) cross-adsorbed conjugated to Alexa Fluor 488, anti-mouse IgG(H+L) cross-adsorbed conjugated to Alexa Fluor 546, and anti-sheep IgG (H+L) cross-adsorbed conjugated to Alexa Fluor 647. The detailed process is described in Ref. [23]. Fluorescence was detected using a confocal auto-fluorescence microscope (Nikon A1R). The excitation and emission wavelengths collected included 487 nm excitation (emission collected between 500–550 nm), 561 nm excitation (emission collected between 570–620 nm), and 639 nm excitation (emission collected between 663–738 nm) for OPN, RPTF-1, and Cal-A, respectively. Auto-fluorescence (AF) was observed from a portion of each sample, but the signal intensity was far lower than the protein signals discussed in this study. In addition, the

binding of antibodies not specific to the target proteins was evaluated, and the absence of IF signals from the non-specific antibodies were confirmed. Negative control tests were performed to assess the absence of false-positive signals, and these data are also shown in Ref. [23]. For antibody staining, isotype controls were used to detect any non-specific binding. Specifically, the primary antibodies used for the controls were rabbit (DA1E) mAb IgG XP isotype control (1:100 dilution; Cell Signaling), mouse (G3A1) mAb IgG1 isotype control (1:100 dilution; Cell Signaling), and sheep mAb IgG isotype (1:100 dilution; Novus) antibodies, and the fluorescently labeled secondary antibodies were the same as described above.

Results

Traces of phase transition inside the CaOx kidney stones

According to the report of Schubert et al. (1981), domains of the kidney stone samples were categorized into three types of textures: an irregular texture composed of euhedral COD crystals (Type 1, referred to as euhedral COD aggregate), a mosaic texture composed of irregular oriented COM crystals (Type 2, referred to as mosaic COM), and a texture made up of concentrically laminated COM crystals (Type 3, referred to as concentric COM).[16] In the center area of sample 1003-9, some concentric COMs (Type 3) were observed (white arrows in Fig. 2 (a)). The concentric COMs had striped patterns at intervals of several mm, in correspondence with previous reports. [16] [15] FTIR spectra showed that the crystal phase of the concentric COMs was almost COM crystals (80±10 %) (Fig. S1(a) and (b)①). When analyzing

the FTIR spectrums, we ignored the organic contents incorporated in the texture and considered only mineral phases; the COM/COD ratio was determined by the method in Ref.[27]. We observed the mosaic COM texture around the outside perimeter of the concentric COMs. Figure 2(b) and (c) are magnified images of the mosaic COMs. The FTIR spectrums of this texture also showed that the main mineral phase was COM, and the ratio was nearly 100% (Fig. S1 (a) and (b)②, ③). Many voids existed in the mosaic structure. The outer region of the sample had a texture with characteristic, outwardly projecting points. The angles of the points were acute, about 50 – 60 degrees, and they were similar to the shape of euhedral COD (Type 1). However, despite the similarity between the external form of the textures and euhedral CODs, the interior of the points consisted of mosaic COMs. At the edge of the pointed texture, COMs and, locally, CODs were confirmed by the FTIR spectrum (Fig. S1 (a) and (b) ④).

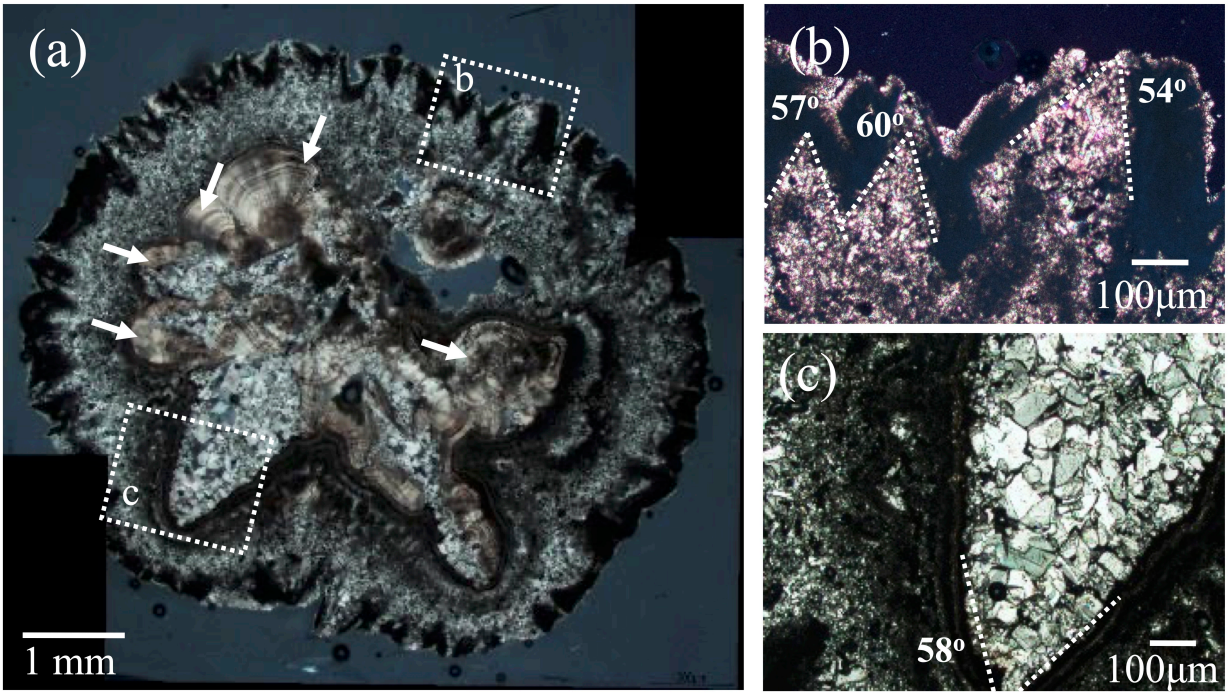

Figure 2. Cross-Nicol images of sample 1003-9. (a) An overall appearance of the stone. (b) Enlarged image of the dashed square b in (a). (c) Enlarged image of the dashed square c in (a).

Observation of internal structure and crystal phase of kidney stones by a microfocus X-ray CT system

We picked up samples 1010-2 and 1011 as typical COD kidney stones, then observed them using a microfocus X-ray CT system (microfocus X-ray CT). Sample 1010-2 appeared to be a several-millimeter COD single crystal. Two tiny COD crystals adhered to the crystal surface (Fig. 3 (a)). Sample 1011 was composed of multiple COD crystals joined together (Fig. 3 (b)). COD crystals are known to have a tetragonal bipyramid shape formed of {101} faces.[28] The samples 1010-2 and 1011 also showed clear {101} faces.

Figures 3 (c) and (d) are the X-ray CT images. The CT values inside the COD crystals were not uniform; light-gray, gray and black regions were observed. The CT values corresponded to the X-ray linear attenuation coefficient of each crystal phase. Zarse et al. reported that the CT value of COM ranged from 16297 to 18449 AU, COD ranged from 13815 to 15797 AU, and calcium phosphate ranged from 21144 to 23121 AU. [29] [30] The edge of sample 1010-2 was mainly composed of COD (dark gray). Combined COM crystals (gray color) existed at the center. We could observe the alternate layers of the COD main region and the COM tiny crystals region from center to edge. The size of the tiny COM crystals was ~several tens of micrometers, and many voids existed around the crystals. In the case of sample 1011, crystals also had gray and dark gray areas, which corresponded to COM and COD. Each crystal had a COD rim area, and there were many tiny COM crystals with voids inside.

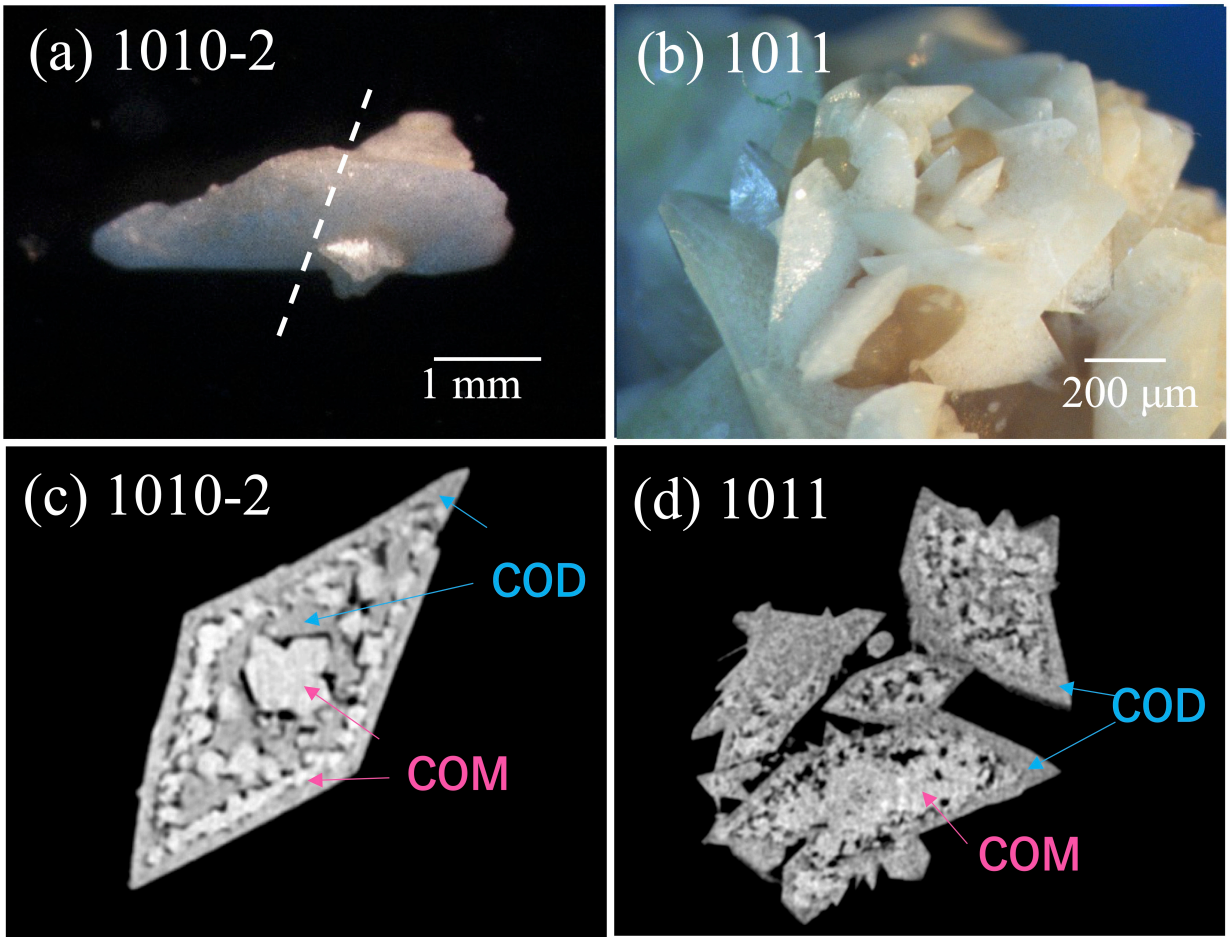

Figure 3. Images of kidney stones mainly composed of COD crystals. (a) An image of Sample 1010-2. (b) An image of Sample 1011. (c),(d) Microfocus X-ray CT images of Sample1010-2 and Sample 1011.

Visualization of protein distribution inside crystals by Multi-IF staining

Figure 4 (a) and (e) are open-Nicol images of euhedral COD (Type 1) and mosaic COM (Type 2). Figure (b)-(d) and (f)-(h) are Multi-IF staining images of euhedral COD (Type 1) and mosaic COM (Type 2). As shown by Ref.[23], OPN and RPTF-1 were distributed along the crystal striation in Type 1. OPN (Fig. 4 (c)) and RPTF-1(Fig. 4 (d)) tended to concentrate in different

crystallographic orientations, but both exhibited periodic distributions according to the crystal growth process. Figure 4 (i) shows the intensities of OPN (line A-A'), and those of RPTF-a (line B-B'). We can see periodic strength. OPN and RPTF-1 were also present inside the mosaic-like COM (Type 2), but neither showed the apparent striations seen in Type 1, and they were confirmed to have a nearly uniform concentration inside the crystal grains (Fig. 4 (f)-(h)). Figure 4 (j) shows the intensities of OPN and RPTF-1, along the line C-C'. Two strong intensities were observed along cracks (arrows in Fig. 4 (j)), but the distributions of OPN and RPTF-a were relatively uniform in other areas compared to Fig. 4 (i). Weak striations were confirmed inside the other crystal, as indicated by the dashed white square in Fig. 4 (f). The intensities of OPN and RPTF-1 along line D-D' are shown in Fig. 4 (k). We can see weak periodic contrasts of RPTF-1, but they are not noticeable compared to Fig. 4 (j).

In Ref.[23], we reported the distribution of three different proteins in concentric COM (Type 3). It is apparent that in the concentric COM, clear striations exist (Fig.5).

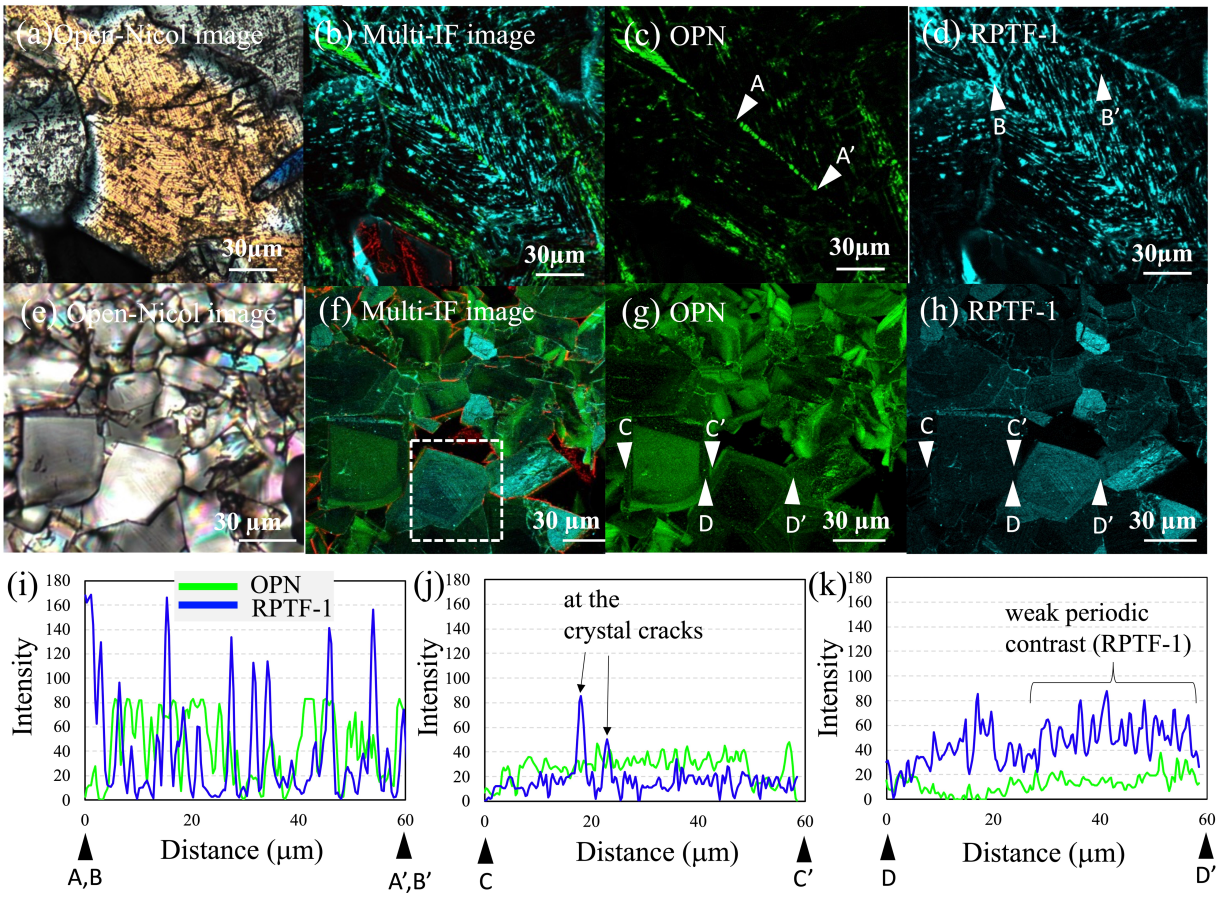

Figure 4. (a)-(d) Protein distributions in a euhedral COD. (a) Open-Nicol image, (b) Multi-IF image. OPN appears in Green, RPTF-1 in blue, and Calgranulin-A in Red. (c) IF image of OPN. OPN preferentially distribute on{110}. (d) IF image of RPTF-1. RPTF-1 preferentially distribute on {101}. (e)-(h) Protein distributions in mosaic COM aggregates. (e) Open-Nicol image, (f) Multi-IF image. OPN appears in Green, RPTF-1 in blue, and Calgranulin-A in Red. (g)IF image of OPN, (h) IF image of RPTF-1. (i) OPN intensity along line A-A' in (c) and RPTF-1 intensity along line B-B' in (d). (j) OPN intensity along line C-C' in (g) and RPTF-1 intensity along line C-C' in (h). (k) OPN intensity along line D-D' in (g) and RPTF-1 intensity along line D-D' in (h).

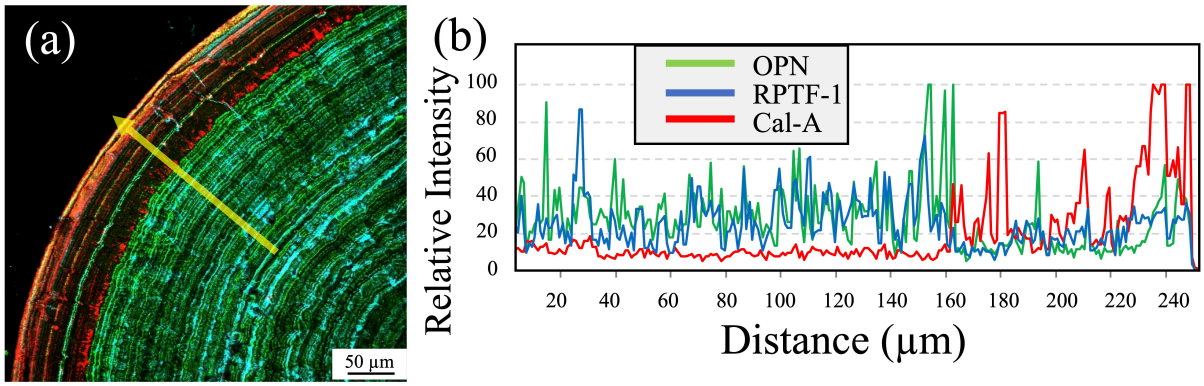

Figure 5. (a) Multi-IF image of concentrically laminated COM (Type 3). Calgranulin-A appears in Red, OPN in Green, and RPTF-1 in blue. (b) Line intensity profiles across the concentric COM in (a). Reprinted with permission from *Scientific Reports* Ref. [23]. Copyright 2021, Springer Nature.

Discussion

Phase transition within kidney stone samples

Pseudomorphs are often found in the natural environment. The outline of the pseudomorphs becomes the shape of the primary mineral. However, while maintaining its outer shape, the primary mineral gradually undergoes a phase transition to another crystal phase and finally becomes an entirely different crystal phase. As a result, certain crystalline phases exhibit geometries that cannot exist in crystallographic morphologies. For example, Momma et al. discovered crystallographically impossible morphology quartz in natural environments. They

focused on whether it was a pseudomorph of a different crystal phase, and conducted a detailed analysis. As a result, they discovered *chibaite* as a new mineral.[31]

Like the discovery, based on the crystal textures and phases inside the kidney stone in Fig. 2, we assumed that the 1003-9 stone was initially composed of multiple euhedral COD crystals (Type 1) bonded around the concentric COM crystals (Type 3). Then, we hypothesized that euhedral COD crystals gradually transformed into tiny COM crystals whose interiors were replaced with mosaic COM crystals (Type 2) while maintaining the shape of the COD single crystals. Of course, it is currently impossible to observe in real-time how crystals generate, grow and aggregate, and then undergo the phase transition in the body. However, it is possible to conduct detailed observations of kidney stones in the intermediate reaction process in order to investigate our hypothesis.

The results in Fig. 3 support our hypothesis. This is an intermediate process in which the inside of euhedral COD crystals was successively replaced with tiny COM crystals. Comparing samples 1010-2 and 1011, 1010-2 is closer to the initial stage of the reaction and has a higher percentage of COD remaining inside the stone. On the other hand, sample 1011 is considered to be from a stone in which the reaction had progressed further, so that the stone interior was almost entirely replaced by COM crystals, leaving the marginal part as COD. In addition, there were voids inside the stone. Similar results were observed by Sivaguru and colleagues: they reported that when the phase transitions from COD to COM, the volume decreases due to water loss, and voids are formed inside the stone.[15] Thus, it is reasonable to

assume that such a phase transition occurs continuously, eventually resulting in a structure almost replaced by a mosaic structure of COM.

The results of Multi-IF staining in Fig. 4 directly support the above phase transition model. The striations generated inside the COD crystal were distinct and periodic, so they were affected by changes in the environment in which the crystal grew. Although it was unclear what occasional fluctuations were involved, daily and/or seasonal fluctuations are conceivable. For example, the amount of osteopontin secreted in the body does not fluctuate significantly daily, but the amount of produced urine differs between day and night.[32] In addition, daily urine output varies between summer and winter.[33] [34] Urinary protein tends to be concentrated during periods of low urine output,[32] so it is possible that these daily or seasonal variations cause distinct striations. It will be necessary to determine which fluctuations dominantly affect the concentration of proteins in COD crystals, considering, for example, the growth rate of crystals. Unfortunately, we do not have enough data to reach a conclusion at present, but plans to study this issue are underway at our laboratory.

On the other hand, almost no striations were visible in mosaic-like COMs. For example, in the COMs in Fig. 4(f)-(h), OPN and prothrombin appeared homogeneously distributed inside the crystal (e.g., along line C-C'; Fig. 4 (k)). In some COMs, protein-rich areas existed along cracks inside the crystal, but no apparent periodic striations were observed. In the white square in Fig. 4 (f), weak striations can be seen inside the COM crystal (along line D-D'; Fig. 4 (k))), but they are less clear than the striations in the COD seen in Fig. 4 (b)-(d). These results

suggest that the observed mosaic COMs grew in locations less susceptible to periodic concentration fluctuations in urine, at least compared to CODs.

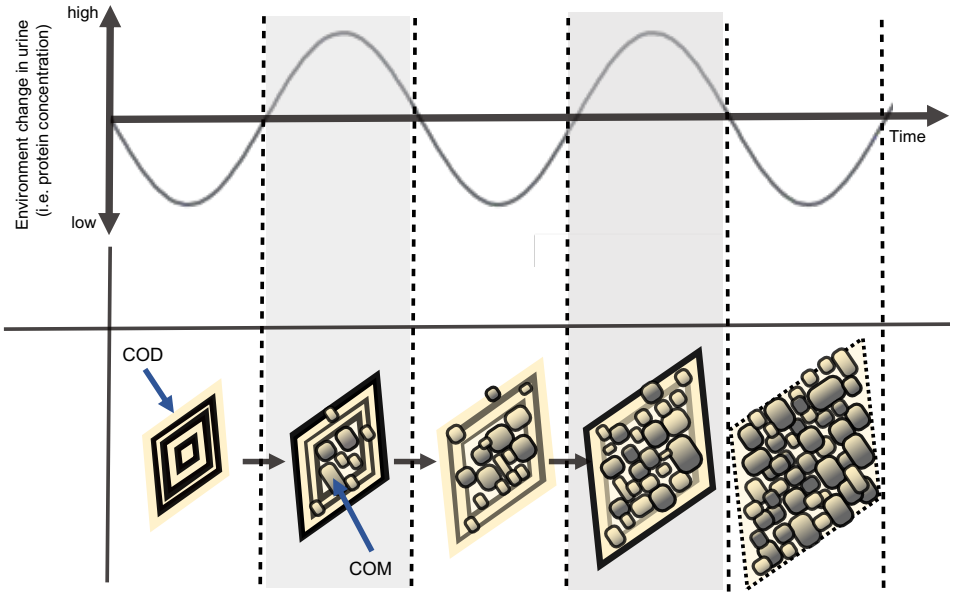

Figure 6. Schematic of the process of euhedral COD crystal growth and solution-mediated transformation from a COD crystal to COM crystals corresponding to the periodic environmental change in urine e.g., protein concentration fluctuation.

Stones are constantly exposed to urine as they grow in the urinary tract. This raises a question: Which sites in the urinary tract are not subjected to periodic fluctuations in urine concentration? One answer is within the COD single crystals themselves, as seen in the results in Fig. 3. Generally, crystals have various defects. Inclusions, one of the crystal defects formed by entraining solutions inside the crystal, are often seen in natural crystals. The solution concentration taken into the inclusion will become the equilibrium concentration for the host

crystal (in this case, the COD crystal) and is maintained within the crystal. Suppose no other crystalline phases form within the inclusions, and the temperature of the environment in which the COD crystals are present does not change. In that case, the solution in the inclusions will continue to exist. However, when COM crystals nucleate inside these inclusions, or when COM microcrystals are initially contained in the inclusions, the phase transition is initiated through the solution. According to Ref. [35], the solubility of COD is always higher than that of COM in the human body environment. In other words, the equilibrium condition for COD is supersaturated for COM, and the growth of COM crystals can proceed. As the COM crystals grow and the solution concentration in the inclusion decreases, the COD crystals that make up the inclusion dissolve until they are in equilibrium with the solution. However, Ca ions and oxalate ions increased by the dissolution of the COD crystal are quickly used for the growth of COM crystals through the solution in inclusions. In this way, a solution-mediated phase transition occurs in which the dissolution of COD crystals and the growth of COM crystals arise continuously. This reaction continues up to an environment where supersaturated conditions are maintained for the COD crystals at all times; this supersaturated environment is near the interface where the COD crystals come into contact with urine.

Considering the average calcium ion concentration and oxalate ion concentration in urine, urine is always a supersaturated environment with COM and COD concentrations several times higher than those at equilibrium. Therefore, when the COM crystal grows near the periphery of the COD crystal by the solution-mediated phase transition, it reaches the interface where the COD crystal continues to grow, so the COD crystal tends to remain in the

periphery part. Alternatively, the COD crystal grown in vivo contains inclusions and defects such as cracks. If the inclusion interface progresses to the vicinity of the outermost shell of COD, inclusions may become a semi-open system through cracks. The phase transition from COD to COM would be slowed in such an environment. The low-contrast striations surrounded by the dashed lines in Fig. 4 (f) were probably affected by the protein concentration distribution in the COD crystal. Partial crystal dissolution of COD during the phase transition produces slight protein concentration fluctuation due to the protein distribution inside the COD crystal. The grown COM crystal might have been affected by such a slight concentration change.

Another possible environment in which stones can dissolve in the urinary tract is near the center of a growing stone. A kidney stone forms through crystal nucleation, growth, aggregation, and calcification. Crystals aggregate and are tightly packed near the central part of a stone. Thus the central area is like a semi-closed system, making it difficult for urine to come into the center easily. Once COM crystal growth begins, the phase transition interface gradually moves from the interior to the exterior of the stone. The transformation stops or significantly slows down at sites where the supply of solutes from urine and the consumption of solutes by COM growth are balanced. In fact, there are many cases of kidney stones that are formed of COD crystals in the outer part but contain COM crystals in the center [14]. We also speculate that a kidney stone we reported in Ref. [27] was also formed by this process.

The contact-mediated transition may be also possible inside of a kidney stone. However, we consider the solution-mediated phase transition as the main process. The result of Fig.4

supports the consideration; it is speculated that protein striations may remain more apparent than those observed in this study when the contact-mediated transition occurs in a solution-free environment. The second piece of evidence is that the coexistence of COM and COD is maintained for several years or more when surgically removed stones are stored in the air. The contact-mediated phase transition may progress gradually, even without a solution, but at least it is considered a prolonged phenomenon. In addition, water molecules are released during the phase transition from COD to COM. Although the amount may be minute, the presence of such water promotes a local solution-mediated phase transition.

How does the phase transition from COD to COM affect the stone formation process?

In the crystal nucleation process, the metastable phase preferentially nucleates when the solution concentration is supersaturated for both the stable and metastable phases (Ostwald's step rule) [18]. This is because metastable phases with higher solubility have lower interfacial energies than stable forms[36] [37]. According to the classical nucleation theory, the metastable phases with low interfacial energies nucleate more readily [38] [39]. Indeed, some examples have been reported in studies on the crystallization of pharmaceutical compounds. [40] [41] [42] COM and COD are pseudo-polymorphs. Preferential nucleation of the metastable phase holds for COM and COD nucleation in the urinary tract. In other words, COD nuclei are likely to form in the urine. Nucleated and crystallized COD single crystals in the urinary tract where there is sufficient space exhibit idiomorphism. In fact, many CODs found in kidney stones exhibit idiomorphism, such as Type 1, and this can also be regarded as indirect evidence of preferential

nucleation of CODs. The high nucleation frequency of the metastable phase and direct COM nucleation "effectively" facilitate the nucleation process in stone formation.

Next, we will consider the effect of solution-mediated phase transition on the velocity of kidney stone growth. Aggregates of COD have a texture in which relatively coarse crystals are gathered, and voids are present. As described in the Results section and the first part of the Discussion section (see **Phase transition within kidney stone samples)**, such a COD stone undergoes the solution-mediated phase transition from inside the COD single crystal or the core of the stone, and gradually changes to COM. In some cases, the reaction proceeds faster than the direct COM stone formation. Because the components that make up COM crystals (Ca^{2+} and $C_2O_4^{2-}$) are already concentrated in the form of COD, so as long as COD remains, a high degree of supersaturation is maintained locally for COM. Such a phenomenon has also been reported for other biominerals, and is a highly effective strategy for creating crystal structures that are convenient for living organisms.[43] [44] [45] On the other hand, in diseases such as urinary calculi, vascular calcification, and gout, it is a very troublesome mechanism that promotes disease progression.

The solution-mediated phase transition probably produces a dense and rigid COM mosaic structure. This is because COMs gradually replace and fill a limited space—i.e., a COD single crystal or an aggregate of dense CODs—by phase transition. In such a process, areas in the stone are effectively packed. As mentioned in the results of Fig. 4, some proteins inside the COD crystals are also released during COM growth and affect the process, so the COM crystals

formed by the phase transition may stick together through the binding of certain specific proteins. Finally, a COM stone created in this way would be a troublesome stone that would be difficult to split by surgeries.

In consideration of all the above, the solution-mediated phase transition from COD to COM greatly facilitates the processes of crystal nucleation, growth, aggregation, and calcification. The rate of the solution-mediated phase transition may be slowed when the exposure of the stone to the urine is limited, such as when the stone blocks the urethra. Still, the phase transition will gradually progress from the point exposed to urine. The environment in which the kidney stone is located possibly lead to unevenness in the progress of the phase transition inside the stone. Actually, some stones have both local mosaic COM and idiomorphic COD within the same stone. By focusing on the difference in the degree of phase transition inside the calculus, it may be possible to decipher what kind of environment the calculus has stayed in for a long time. It will be essential to investigate the crystal components and crystal phases of kidney stones expelled from patients, and to collect data on the difference in the probability of subsequent recurrence in the case of a stone with evidence of the phase transition. Such information may be helpful in accurately predicting the timing of recurrence. In addition, if the metastable-to-stable phase transition mechanism can be stopped, it may be possible to prevent the formation of stones that are difficult to crush during surgery. Therefore, it is crucial to elucidate the phase transition mechanism in kidney stones and search for new treatment strategies.

Conclusions

In this study, we analyzed sections of kidney stones that had been expelled from the bodies of patients with kidney stone disease. Pseudomorph structures were often found inside the kidney stones, and partial COM crystals inside COD single crystals were shown to be a clear trace of the solution-mediated phase transition from COD stones to COM stones. In addition, the visualization of the protein distribution in the kidney stones supported the fact that euhedral COD crystals (Type 1) and concentric COM (Type 3) were the primary phase and that most mosaic COM crystals (Type 2) were the secondary phase. The crystal phase transition from COD to COM efficiently promotes crystal nucleation, crystal growth, aggregation, and calcification in kidney stone formation. For this reason, it is crucial to confirm the traces of solution-mediated phase transition for each patient to predict the possibility and timing of recurrence.

Supporting information

Supporting information is available.

Figure SI. Cross-Nicol image of sample 1003-9 and FTIR spectra of the sample.

Acknowledgments

We thank K. P Sawada and R. Mori for their observation and experiments. We thank K. Murakami, H. Kubo and K. Kawamura for their experimental support. We also thank the members of the Medical and Engineering Tactics for Elimination of Rocks (METEOR) Project for their helpful discussions. Part of this study was supported by the JSPS KAKENHI Grant-in-Aid for Scientific Research (No. 20K21658 and 22H01971). This work was also supported by the Konica Minolta Science and Technology Foundation, Shiseido Female Researcher Science Grant, Caterpillar STEM award 2019, Kao Crescent award 2022, UHA Mikakuto and the Osaka University Program for the Support of Networking among Present and Future Researchers for M. M. This work was supported in part by Grants-in-Aid for Scientific Research from the Ministry of Education, Culture, Sports, Science, and Technology, Japan (No. 20K21658), the Naito Foundation, and the Hori Sciences and Arts Foundation.

References

(1) Khan, S. R.; Pearle, M. S.; Robertson, W. G.; Gambaro, G.; Canales, B. K.; Doizi, S.; Traxer, O.; Tiselius, H.-G. Kidney stones. *Nature reviews. Disease primers* **2016**, *2*, 16008-16008. DOI: 10.1038/nrdp.2016.8 PubMed.

(2) Pak, C. Y. C. Kidney stones. *THE LANCET* **1998**, *351*, 1797-1801. DOI: 10.1016/S0140-6736(98)01295-1.

(3) Romero, V.; Akpinar, H.; Assimos, D. G. Kidney stones: a global picture of prevalence, incidence, and associated risk factors. *Rev Urol* **2010**, *12* (2-3), e86-e96. PubMed.

(4) Alelign, T.; Petros, B. Kidney Stone Disease: An Update on Current Concepts. *Adv Urol* **2018**, *2018*, 3068365-3068365. DOI: 10.1155/2018/3068365 PubMed.

(5) Herring, L. C. Observations on the analysis of ten thousand urinary calculi. *J Urol* **1962**, *88*, 545-562. DOI: 10.1016/s0022-5347(17)64842-0 From NLM.

(6) Daudon, M.; Bader, C.; Jungers, P.; Beaugendre, O.; Hoarau, M. Urinary calculi: review of classification methods and correlations with etiology. *Scanning Microscopy* **1993**, *7* (3), 32.

(7) Daudon, M.; Dessombz, A.; Frochot, V.; Letavernier, E.; Haymann, J.-P.; Jungers, P.; Bazin, D. Comprehensive morpho-constitutional analysis of urinary stones improves etiological diagnosis and therapeutic strategy of nephrolithiasis. *Comptes Rendus Chimie* **2016**, *19*. DOI: 10.1016/j.crci.2016.05.008.

(8) Gehl, A.; Dietzsch, M.; Mondeshki, M.; Bach, S.; Häger, T.; Panthöfer, M.; Barton, B.; Kolb, U.; Tremel, W. Anhydrous Amorphous Calcium Oxalate Nanoparticles from Ionic Liquids: Stable Crystallization Intermediates in the Formation of Whewellite. *Chemistry – A European Journal* **2015**, *21* (50), 18192-18201. DOI: 10.1002/chem.201502229.

(9) Tazzoli, V.; Domeneghetti, C. The crystal structures of whewellite and weddellite: re-examination and comparison. *American Mineralogist* **1980**, *65* (3-4), 327-334. (acccessed 2/18/2021).

(10) Momma, K.; Izumi, F. VESTA 3 for three-dimensional visualization of crystal, volumetric and morphology data. *Journal of Applied Crystallography* **2011**, *44* (6), 1272-1276. DOI: 10.1107/s0021889811038970.

(11) Chien, Y.-C.; Mansouri, A.; Jiang, W.; Khan, S. R.; Gray, J. J.; McKee, M. D. Modulation of calcium oxalate dihydrate growth by phosphorylated osteopontin peptides. *Journal of Structural Biology* **2018**, *204* (2), 131-144. DOI: https://doi.org/10.1016/j.jsb.2018.07.010.

(12) Miyazawa, K.; Suzuki, K. Urolithiasis Clinical Practice Guideline 2013. *The Journal of the Japanese Society of Internal Medicine* **2017**, *106* (5), 994-999. DOI: 10.2169/naika.106.994.

(13) Moriguchi, H.; Hara, Y.; Tozuka, K.; Tokue, A. Estimation of the weddellite to whewillite ratio by infrared spectroscopy. *Acta Urologica Japonica* **1991**, *37,* 1-5. http://hdl.handle.net/2433/117098.

(14) Bazin, D.; Leroy, C.; Tielens, F.; Bonhomme, C.; Bonhomme-Coury, L.; Damay, F.; Le Denmat, D.; Sadoine, J.; Rode, J.; Frochot, V.; et al. Hyperoxaluria is related to whewellite and hypercalciuria to weddellite: What happens when crystalline conversion occurs? *Comptes Rendus Chimie* **2016**, *19* (11), 1492-1503. DOI: https://doi.org/10.1016/j.crci.2015.12.011.

(15) Sivaguru, M.; Saw, J. J.; Williams, J. C.; Lieske, J. C.; Krambeck, A. E.; Romero, M. F.; Chia, N.; Schwaderer, A. L.; Alcalde, R. E.; Bruce, W. J.; et al. Geobiology reveals how human kidney stones dissolve in vivo. *Scientific Reports* **2018**, *8* (1), 13731. DOI: 10.1038/s41598-018-31890-9.

(16) Schubert, G.; Brien, G. Crystallographic investigations of urinary calcium oxalate calculi. *International Urology and Nephrology* **1981**, *13* (3), 249-260. DOI: 10.1007/BF02082422.

(17) Grases, F.; Costa-Bauzá, A.; García-Ferragut, L. Biopathological crystallization: a general view about the mechanisms of renal stone formation. *Advances in Colloid and Interface Science* **1998**, *74* (1), 169-194. DOI: https://doi.org/10.1016/S0001-8686(97)00041-9.

(18) Ostwald, W. Studien über die Bildung und Umwandlung fester Körper:. *Z. Phys. Chem.* **1897**, *22*, 289-330.

(19) Zhang, J.; Wang, L.; Putnis, C. V. Underlying Role of Brushite in Pathological Mineralization of Hydroxyapatite. *J Phys Chem B* **2019**, *123* (13), 2874-2881. DOI: 10.1021/acs.jpcb.9b00728 From NLM.

(20) Díaz-Soler, F.; Rodriguez-Navarro, C.; Ruiz-Agudo, E.; Neira-Carrillo, A. Stabilization of Calcium Oxalate Precursors during the Pre- and Post-Nucleation Stages with Poly(acrylic acid). *Nanomaterials* **2021**, *11* (1), 235.

(21) Putnis, C. V.; Ruiz-Agudo, E. Nanoparticles formed during mineral-fluid interactions. *Chemical Geology* **2021**, *586*, 120614. DOI: https://doi.org/10.1016/j.chemgeo.2021.120614.

(22) Tajiri, R.; Fujita, T. Observation methods of hard and soft animal tissues. *TAXA, Proceedings of the Japanese Society of Systematic Zoology* **2013**, *35*, 24-34.

(23) Tanaka, Y.; Maruyama, M.; Okada, A.; Furukawa, Y.; Momma, K.; Sugiura, Y.; Tajiri, R.; Sawada, K. P.; Tanaka, S.; Takano, K.; et al. Multicolor imaging of calcium-binding proteins in human kidney stones for elucidating the effects of proteins on crystal growth. *Scientific Reports* **2021**, *11* (1), 16841. DOI: 10.1038/s41598-021-95782-1.

(24) Williams, J. C., Jr.; Worcester, E.; Lingeman, J. E. What can the microstructure of stones tell us? *Urolithiasis* **2017**, *45* (1), 19-25. DOI: 10.1007/s00240-016-0944-z PubMed.

(25) Shimadzu Application Note. Kramers-Kronig Transform and Applications [cited 2023 1/18]. Shimadzu C103-E031. Available from: chrome-extension://efaidnbmnnnibpcajpcglclefindmkaj/https://shimadzu.com.au/sites/default/files/Appl_FTIR_Polymer_specular_reflectance_055_en.pdf. (accessed 2023 1/18).

(26) Maruyama, M.; Sawada, K. P.; Tanaka, Y.; Okada, A.; Momma, K.; Nakamura, M.; Mori, R.; Furukawa, Y.; Sugiura, Y.; Tajiri, R.; et al. Quantitative analysis of calcium oxalate monohydrate and dihydrate for elucidating the formation mechanism of calcium oxalate kidney stones. *PLOS ONE* **2023**, *18* (3), e0282743. DOI: 10.1371/journal.pone.0282743.

(27) Maruyama, M.; Yoshikawa, H. Y.; Takano, K.; Yoshimura, M.; Mori, Y. Solution-mediated phase transition of pharmaceutical compounds: Case studies of acetaminophen and aspirin. *Journal of Crystal Growth* **2023**, *602*, 126990. DOI: https://doi.org/10.1016/j.jcrysgro.2022.126990.

(28) Debroise, T.; Sedzik, T.; Vekeman, J.; Su, Y.; Bonhomme, C.; Tielens, F. Morphology of Calcium Oxalate Polyhydrates: A Quantum Chemical and Computational Study. *Crystal Growth & Design* **2020**, *20* (6), 3807-3815. DOI: 10.1021/acs.cgd.0c00119.

(29) Zarse, C. A.; McAteer, J. A.; Sommer, A. J.; Kim, S. C.; Hatt, E. K.; Lingeman, J. E.; Evan, A. P.; Williams, J. C. Nondestructive analysis of urinary calculi using micro computed tomography. *BMC Urology* **2004**, *4* (1), 15. DOI: 10.1186/1471-2490-4-15.

(30) Williams, J. C., Jr.; McAteer, J. A.; Evan, A. P.; Lingeman, J. E. Micro-computed tomography for analysis of urinary calculi. *Urol Res* **2010**, *38* (6), 477-484. DOI: 10.1007/s00240-010-0326-x From NLM.

(31) Momma, K.; Ikeda, T.; Nishikubo, K.; Takahashi, N.; Honma, C.; Takada, M.; Furukawa, Y.; Nagase, T.; Kudoh, Y. New silica clathrate minerals that are isostructural with natural gas hydrates. *Nature Communications* **2011**, *2* (1), 196. DOI: 10.1038/ncomms1196.

(32) Min, W.; Shiraga, H.; Chalko, C.; Goldfarb, S.; Krishna, G. G.; Hoyer, J. R. Quantitative studies of human urinary excretion of uropontin. *Kidney International* **1998**, *53* (1), 189-193. DOI: https://doi.org/10.1046/j.1523-1755.1998.00745.x.

(33) Kawamura, M.; Hashimoto, T.; Ogino, T.; Kaneko, H.; Mifune, S.; Watanabe, T.; Usui, Y.; Tsuchikawa, G.; Shozushima, M.; Kudou, H. Seasonal Variation in the Daily Urinary Sodium Excretion in Outpatients from the Morioka Region of Northern Japan. *Intern Med* **2017**, *56* (11), 1321-1329. DOI: 10.2169/internalmedicine.56.8270 From NLM.

(34) Attalla, K.; De, S.; Sarkissian, C.; Monga, M. Seasonal variations in urinary calcium, volume, and vitamin D in kidney stone formers. *International braz j urol* **2018**, *44*.

(35) Streit, J.; Tran-Ho, L.-C.; Königsberger, E. Solubility of the three calcium oxalate hydrates in sodium chloride solutionsand urine-like liquors. *Monatshefte für Chemie/Chemical Monthly* **1998**, *129* (12), 1225-1236.

(36) Nielsen, A. E.; Sohnel, O. Interfacial tensions electrolyte crystal-aqueous solution, from nucleation data. *Journal of Crystal Growth* **1971**, *11* (3), 233-242.

(37) Söhnel, O.; Mullin, J. W. A method for the determination of precipitation induction periods. *Journal of Crystal Growth* **1978**, *44* (4), 377-382.

(38) Chernov, A. A. *Modern Crystallography III, Crystal Growth,*; Springer, 1984.

(39) Markov, I. *CRYATAL GROWTH FOR BEGINNERS: Fundamentals of Nucleation, Crystal Growth and Epitaxy*; 2003.

(40) Mori, Y.; Maruyama, M.; Takahashi, Y.; Ikeda, K.; Fukukita, S.; Yoshikawa, Y. H.; Okada, S.; Adachi, H.; Sugiyama, S.; Takano, K.; et al. Selective crystallization of metastable phase of acetaminophen by ultrasonic irradiation. *Applied Physics Express* **2015**, *8* (6), 065501.

(41) Ikeda, K.; Maruyama, M.; Takahashi, Y.; Mori, Y.; Yoshikawa, H. Y.; Okada, S.; Adachi, H.; Sugiyama, S.; Takano, K.; Murakami, S.; et al. Selective crystallization of the metastable phase of indomethacin at the interface of liquid/air bubble induced by femtosecond laser irradiation. *Applied Physics Express* **2015**, *8* (4), 045501.

(42) Fujimoto, R.; Maruyama, M.; Okada, S.; Adachi, H.; Yoshikawa, H. Y.; Takano, K.; Imanishi, M.; Tsukamoto, K.; Yoshimura, M.; Mori, Y. Large-scale crystallization of acetaminophen trihydrate by a novel stirring technique. *Applied Physics Express* **2019**, *12* (4), 045503. DOI: 10.7567/1882-0786/ab0666.

(43) Weiss, I. M.; Tuross, N.; Addadi, L.; Weiner, S. Mollusc larval shell formation: amorphous calcium carbonate is a precursor phase for aragonite. *Journal of Experimental Zoology* **2002**, *293* (5), 478-491. DOI: https://doi.org/10.1002/jez.90004.

(44) Xiao, C.; Li, M.; Wang, B.; Liu, M.-F.; Shao, C.; Pan, H.; Lu, Y.; Xu, B.-B.; Li, S.; Zhan, D.; et al. Total morphosynthesis of biomimetic prismatic-type CaCO3 thin films. *Nature Communications* **2017**, *8* (1), 1398. DOI: 10.1038/s41467-017-01719-6.

(45) Huang, J.; Liu, C.; Xie, L.; Zhang, R. Amorphous calcium carbonate: A precursor phase for aragonite in shell disease of the pearl oyster. *Biochem Biophys Res Commun* **2018**, *497* (1), 102-107. DOI: 10.1016/j.bbrc.2018.02.031 From NLM.

For Table of Contents Only

Evidence for solution-mediated phase transitions in kidney stones

-Phase transition exacerbates kidney stone disease-

Mihoko Maruyama*, Yutaro Tanaka, Koichi Momma, Yoshihiro Furukawa, Hiroshi Y. Yoshikawa, Rie Tajiri, Masanori Nakamura, Kazumi Taguchi, Shuzo Hamamoto, Ryosuke Ando, Katsuo Tsukamoto, Kazufumi Takano, Masayuki Imanishi, Shigeyoshi Usami, Kenjiro Kohri, Atsushi Okada, Takahiro Yasui, Masashi Yoshimura, Yusuke Mori

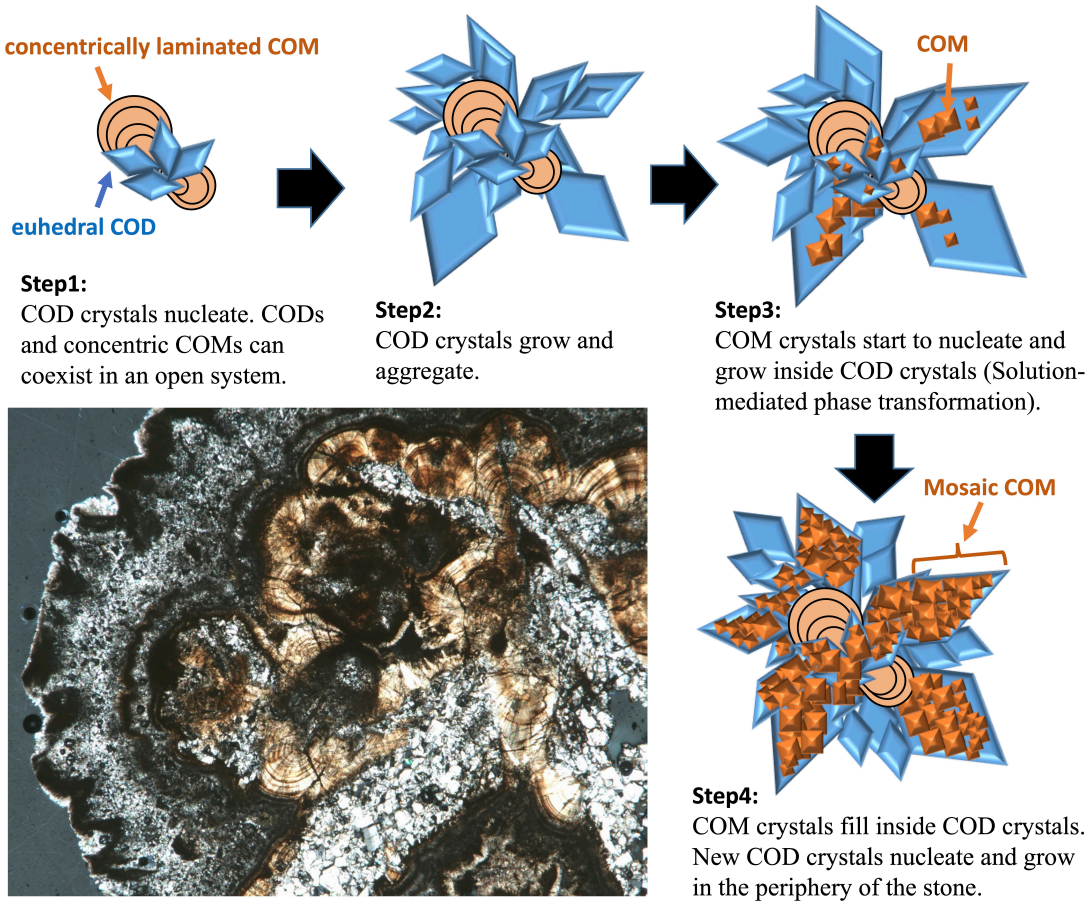

Synopsis

Investigation of calcium oxalate (CaOx) kidney stones showed direct evidence of the solution-mediated phase transition of calcium oxalate dihydrate (COD; the metastable phase) to calcium oxalate monohydrate (COM; the stable phase). The crystal phase transition from COD to COM efficiently promotes crystal nucleation, crystal growth, aggregation, and calcification in kidney stone formation.